Radboud Repository

Radboud University Nijmegen

PDF hosted at the Radboud Repository of the Radboud University Nijmegen

The following full text is a preprint version which may differ from the publisher's version.

For additional information about this publication click this link.
http://hdl.handle.net/2066/174430

Please be advised that this information was generated on 2019-12-31 and may be subject to change.

Journal Name

ARTICLE TYPE

Cite this: DOI: 10.1039/xxxxxxxxxx

Metal diffusion barriers for GaAs solar cells

R.H. van Leest,[a*], P. Mulder[a], G.J. Bauhuis[a], H. Cheun[b], H. Lee[b], W. Yoon[b], R. van der Heijden[c], E. Bongers[c], E. Vlieg[a] and J.J. Schermer[a]

Received Date
Accepted Date

DOI: 10.1039/xxxxxxxxxx

www.rsc.org/journalname

In this study accelerated ageing testing (AAT), J-V characterization and TEM imaging in combination with phase diagram data from literature are used to assess the potential of Ti, Ni, Pd and Pt as diffusion barriers for Au/Cu-based metallization of III-V solar cells. Ni barriers show the largest potential as at an AAT temperature of 250°C both cells with 10 and 100 nm thick Ni barriers show significantly better performance compared to Au/Cu cells, with the cells with 10 nm Ni barriers even showing virtually no degradation after 7.5 days at 250°C (equivalent to 10 years at 100°C at an E_a of 0.70 eV). Detailed investigation shows that Ni does not act as a barrier in the classical sense, i.e. preventing diffusion of Cu and Au across the barrier. Instead Ni modifies or slows down the interactions taking place during device degradation and thus effectively acts as an 'interaction' barrier. Different interactions occur at temperatures below and above 250°C and for thin (10 nm) and thick (100 nm) barriers. The results of this study indicate that 10-100 nm thick Ni intermediate layers in the Cu/Au based metallization of III-V solar cells may be beneficial to improve the device stability upon exposure to elevated temperatures.

1 Introduction

Thin-film III-V solar cells obtained by the epitaxial lift-off (ELO) method [1–9] offer excellent characteristics for implementation in space solar panels [10–12]. However, the harsh space environment (vacuum, UV irradiation, high energy electron and proton irradiation, temperature cycling, etc.) [13] also adds a number of challenges to solar cell and panel design. One of those challenges concerns the thin-film solar cell carrier. The thin-film cell design currently used at Radboud University utilizes a Cu handling and support foil as Cu is relatively cheap, compatible with the chemicals used in solar cell processing and can easily be applied with a number of chemical and physical deposition methods. Unfortunately Cu is also known to diffuse rapidly in most semiconductors [14,15] and it forms mid band gap trap levels [16] that may act as a non-radiative recombination pathway. The extreme space environment (in particular the elevated maximum temperature during temperature cycling) may induce Cu diffusion, thereby severely diminishing the device performance.

As Cu diffusion is exponentially dependent on temperature ($D = D_0\exp(-E_a/kT)$) a temperature accelerated testing procedure can be used to accelerate diffusion. Such a procedure is based on the assumption that exposure for a long period of time to a (relatively) low temperature is equivalent to a short exposure (few days) to a higher temperature. This can be described with the following equation [17]:

$$\frac{t_{op}}{t_{acc}} = \exp\left[\frac{E_a}{k}\left(\frac{1}{T_{op}} - \frac{1}{T_{acc}}\right)\right] \quad (1)$$

in which k is the Boltzmann constant, E_a the activation energy for the degradation process, T_{op} the regular operation temperature, T_{acc} the accelerated test temperature and t_{op} and t_{acc} the exposure times to the corresponding temperatures. Typically such accelerated life-time testing (ALT) procedures include operational conditions (illumination, electrical bias) [18,19]. In order to exclude additional (i.e. non temperature-induced) light- and/or electrically-induced degradation mechanisms these operating conditions were excluded in the test procedure used in this study. In a previous study [20] we used the abbreviation ALT for this test procedure, but as this might be confusing we will refer to the adapted test procedure as accelerated ageing testing (AAT). The main difficulty with this accelerated testing approach is that it requires a known activation energy. For solar cell assemblies (cells with cover glass, interconnections and sometimes by-pass diode) under operating conditions ESA's requirements and standards division advises to use 0.70 eV for calculations or to determine the actual activation energy experimentally [19]. As experimental determination of the activation energy is time consuming and difficult and the system under investigation is intended for space

[a] Radboud University, Institute for Molecules and Materials, Heyendaalseweg 135, 6525 AJ Nijmegen, The Netherlands
[*] Corresponding author, e-mail: L.vanLeest@science.ru.nl
[b] LG Electronics Materials & Devices Advanced Research Institute, 16 Woomyeon-Dong, Seocho-Gu, Seoul 137-724, Korea
[c] Airbus Defence and Space Netherlands B.V., Mendelweg 30, 2333 CS Leiden, The Netherlands

applications the activation energy advised by ESA is assumed to be a reasonable first estimate. With this activation energy of 0.70 eV AAT times can be calculated for different missions. The calculated test times at test temperatures between 150 and 400°C for a geosynchronous orbit mission (GEO, 15 years, maximum 70°C), a low Earth orbit mission (LEO, 10 years, maximum 100°C) and an extreme scenario (extreme, 15 years 100°C) are given in table 1.

Table 1 Calculated accelerated test times for a geosynchronous mission (GEO: 15 years, max 70°C), a low-earth orbit mission (LEO: 10 years, max 100°C) and an extreme scenario (Extreme: 15 years, max 100°C) at accelerated test temperatures between 150 and 400°C for an activation energy E_a of 0.70 eV. Test times were rounded of towards the next half hour/day.

E_a = 0.70 eV

T_{acc} (°C)	GEO	LEO	Extreme
150	62.5 d	278.5 d	1.5 y
200	8.5 d	37.0 d	55.0 d
250	2.0 d	7.5 d	11.0 d
300	10.0 h	2.0 d	3.0 d
350	3.5 h	14.5 h	21.5 h
400	1.5 h	5.5 h	8.5 h

It was found in previous studies that cells with plain Au contacts show little degradation upon exposure to elevated temperatures[21], while significant decreases in device performance can be observed for substrate-based cells with Au/Cu front contacts[21,22]. The significant decreases in V_{oc} observed for these cells point to enhanced non-radiative recombination via Cu trap levels. Upon further investigation of the interaction of Cu with the solar cell structure two different degradation mechanisms were identified: at relatively low temperatures (below ∼ 250°C) Au and Cu intermix without any significant effect on the solar cell performance, while at higher temperatures (above ∼ 250°C) the metals start to recrystallize with the GaAs contact layer. This recrystallization process creates large crystallites separated by grain boundaries via which Cu can diffuse rapidly into the active solar cell device, thereby causing the observed decrease in V_{oc}[20]. Although the intermixing of Au and Cu at low temperatures does not have a significant effect on the device performance of substrate-based cells it is still undesirable as intermixing of the Au mirror[3,23,24] and Cu handling foil in a thin-film cell configuration degrades the mirror properties of the Au and thereby the performance of the thin-film solar cells[25].

In order to prevent intermixing of the Cu handling foil and Au mirror and to avoid Cu diffusion into the active solar cell device, a diffusion barrier[26] can be implemented. Metal barriers are preferred as they can be easily implemented in the current thin-film design used at Radboud University. Ti[27,28] and Ni[29–35] are prime candidates as they have already been evaluated as Cu diffusion barriers in Si solar cells. Additionally Pd[36] has been investigated as a diffusion barrier for Cu on GaAs. As Pt is one of the more inert metals and is already implemented in Cu-based metallization schemes for solar cells[37,38] its barrier potential was also evaluated in this work. Application of Pt with the available e-beam evaporation equipment proved to be tricky as a result of the relatively high melting point of Pt. Other metals (in particular Ta) have also been found to be good diffusion barriers[39–41], but unfortunately their high melting points make them unsuitable for application by e-beam evaporation. In this study the diffusion barrier potential of 10 and 100 nm thick Ti, Ni, Pd, and Pt layers was investigated by exposing solar cells with these barriers to prolonged accelerated ageing testing (AAT) at temperatures between 200 and 300°C. The most promising barriers were further investigated by TEM analysis.

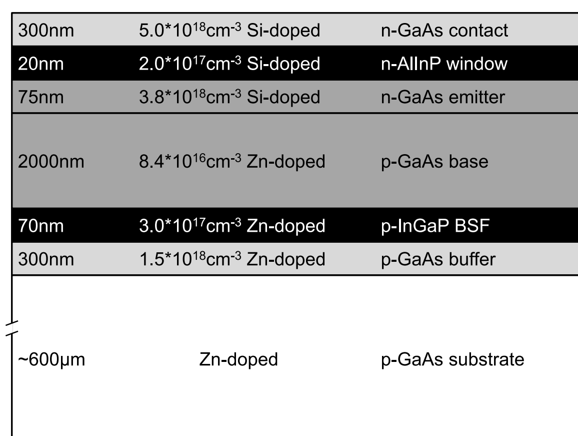

Fig. 1 Schematic representation of the layer structure of the solar cells.

Table 2 Investigated contact metallization schemes.

Contact reference	Layer structure Au	barrier	Cu
Au/Cu	100 nm	–	1 μm
Ti10	100 nm	10 nm Ti	1 μm
Ti100	100 nm	100 nm Ti	1 μm
Ni10	100 nm	10 nm Ni	1 μm
Ni100	100 nm	100 nm Ni	1 μm
Pd10	100 nm	10 nm Pd	1 μm
Pd100	100 nm	100 nm Pd	1 μm
Pt10	100 nm	10 nm Pt	1 μm
Pt100	100 nm	100 nm Pt	1 μm

2 Materials and Methods

A substrate-based model system[21] was used, in which Cu is applied on a 45% coverage front contact. Solar cell structures as schematically depicted in figure 1 were obtained from a third

This journal is © The Royal Society of Chemistry [year]

Table 3 Total AAT times and number of cells subjected to the AAT treatment for AAT temperatures of 200, 250 and 300°C. For each temperature the first two steps represent the equivalent of a GEO mission and all four steps represent the equivalent of a LEO mission for E_a = 0.70 eV.

after	200°C		250°C		300°C		
AAT	total	number	total	number	total	number	mission
step	AAT time	of cells	AAT time	of cells	AAT time	of cells	(E_a = 0.70 eV)
1	4.25 days	4 cells	1 day	4 cells	5 hours	2 cells	
2	8.5 days	4 cells	2 days	4 cells	10 hours	–	GEO
3	22.75 days	2 cells	4.75 days	2 cells	29 hours	–	
4	37 days	2 cells	7.5 days	2 cells	48 hours	–	LEO

party supplier on 4" p-type GaAs wafers. Two of these wafers were cut into 6 pieces and on each of these pieces a set of at least 12 solar cells was prepared. Nine different front contact metallization schemes were investigated. The layer structures and the names these metallization schemes will be referred by are stated in table 2. A barrier free Au/Cu metallization scheme is used as a worst case scenario reference. First a front contact grid with ∼ 45% coverage (a 5.76 mm x 1.66 mm bar with ten 4.08 mm x 160 μm grid fingers spaced 440 μm apart[20,21]) and 100 nm Au back contact were applied by e-beam evaporation. Then 6 mm x 6 mm solar cells were created by a MESA etch, the GaAs layers were etched with a 1:2:10 NH_4OH:H_2O_2:H_2O solution and the AlInP and InGaP layers with a 37% HCl solution. The front contact layer was removed between the grid fingers using a 2:1:10 NH_4OH:H_2O_2:H_2O solution while the metal grid was protected by a layer of photoresist. Finally a 42.5 nm ZnS / 88.0 nm MgF_2 anti-reflection coating was applied by e-beam evaporation. After preparation the cells were characterized by current density-voltage (J-V) measurements, which were obtained with an ABET 2000 Solar Simulator and ReRa Tracer 3.0 software and by external quantum efficiency (EQE) measurements obtained with a ReRa SpeQuest system and ReRa Photor 3.1 software.

The cells were then exposed to stepwise prolonged AAT either at 200°C in a vacuum oven or at 250°C or 300°C in a tube oven under N_2. The total AAT times and number of cells exposed to each AAT step are given in table 3. The first two steps equal a GEO mission and all four steps equal a LEO mission for an E_a of 0.70 eV. For the 200 and 250°C experiments 4 cells were exposed to the first two steps and only 2 of those were exposed to the final two AAT steps. After each step the cells were characterized by J-V and EQE measurements. From the J-V curves before and after each AAT step remaining factors (R) were calculated for the solar cell parameters J_{sc}, V_{oc} and the fill factor (FF) according to:

$$\text{R-parameter} = \frac{\text{parameter value after AAT}}{\text{parameter value as-processed}} . \qquad (2)$$

The remaining factors were then averaged over 2 or 4 cells for each step.

Based on the results of the AAT, cells were selected for transmission electron microscopy (TEM) analysis. These solar cells were covered with a thin Pt protection layer. A cross-section was made and then thinned using focused ion beam milling to allow for cross-sectional TEM analysis of the front contacts. TEM images were obtained with a FEI Titan G2 microscope equipped with EDX analysis tools to determine the composition of the visualized structures.

3 Results and Discussion

3.1 General barrier assessment

In figure 2 the average J_{sc}, V_{oc} and FF remaining factors of cells with various front contact metallization schemes are plotted versus AAT time at T_{acc} = 200°C. The general degradation trends of the Au/Cu cells are indicated by the solid lines. For the Au/Cu cells J_{sc} remains stable (R-J_{sc} approximately 1.00), V_{oc} decreases gradually by 1-2% and FF decreases gradually by 5-10%. This implies that at 200°C cells without a diffusion barrier show virtually no degradation. Therefore no clear conclusions about the barrier potential of Ti, Pt and Ni barriers can be drawn from the 200°C data, as the observed degradation of these cells is similar to the degradation of the diffusion barrier free Au/Cu reference. The most notable deviations from the degradation trends are observed for cells with Pd barriers, which show severe decreases in V_{oc} and FF after 8.5 days and 4.25 days at 200°C for Pd10 and Pd100 cells respectively. Eventually (after 22.75 and 8.5 days for Pd10 and Pd100 cells respectively) the V_{oc} of these cells was found to be effectively zero, making it impossible to obtain useful J-V characteristics. The fact that the cells with Pd eventually show severe cell failure indicates that Pd is not suitable as a barrier material. Additionally the FF of the Ni100 cells deviates from the trend observed for Au/Cu cells. Initially a rapid decrease is observed after which it stabilizes, resulting in an R-FF value of 0.82 after 37 days at 200°C.

Figure 3 shows the average J_{sc}, V_{oc} and FF remaining factors of cells with various front contact metallizations plotted versus AAT time at T_{acc} = 250°C. Already after 1 day at 250°C severe cell failure ($V_{oc} \approx 0$ mV) was observed for cells with Pd barriers, these results are therefore not plotted. The Au/Cu cells display very different degradation trends compared to the trends observed at T_{acc} = 200°C. The J_{sc} of the Au/Cu cells remains stable, V_{oc} initially decreases gradually then drops rapidly (after ∼ 1-2 days) to stabilize at an R-V_{oc} value of approximately 0.2 and FF initially shows a rapid drop followed by a a more gradual decrease to an R-FF

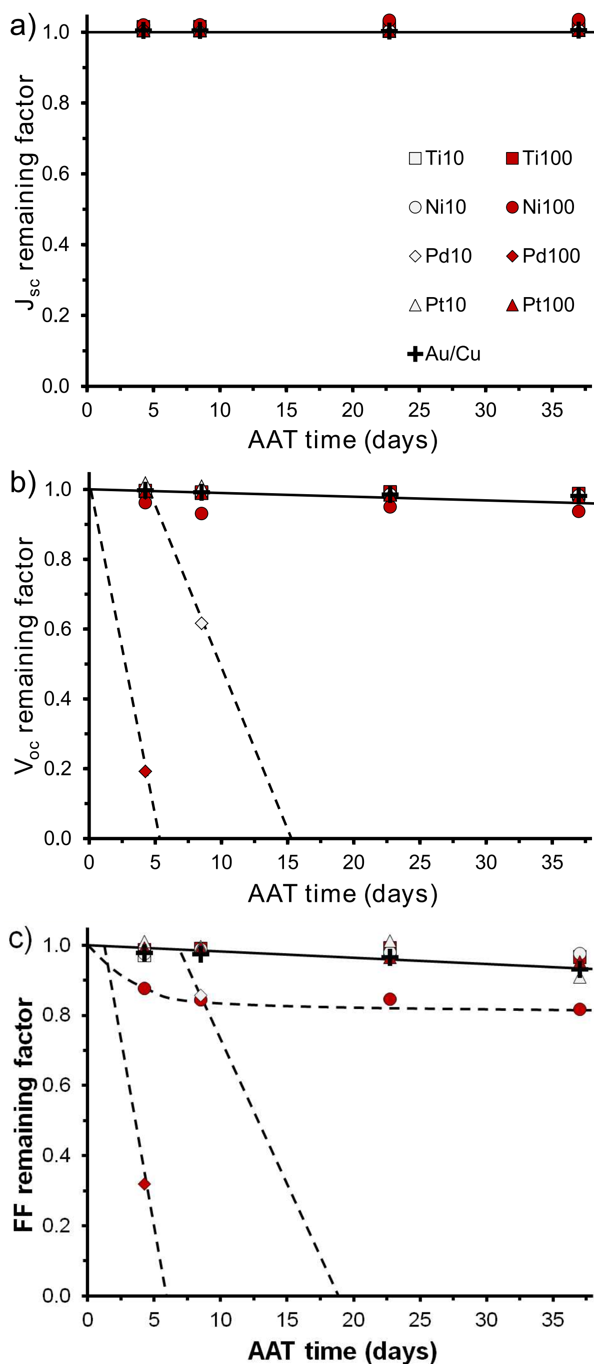

Fig. 2 Average a) J_{sc}, b) V_{oc} and c) FF remaining factors of cells with various front contact metallization schemes plotted versus AAT time at 200°C. The black lines indicate the general degradation trends of the Au/Cu cells and the dashed lines indicate the most notable deviations.

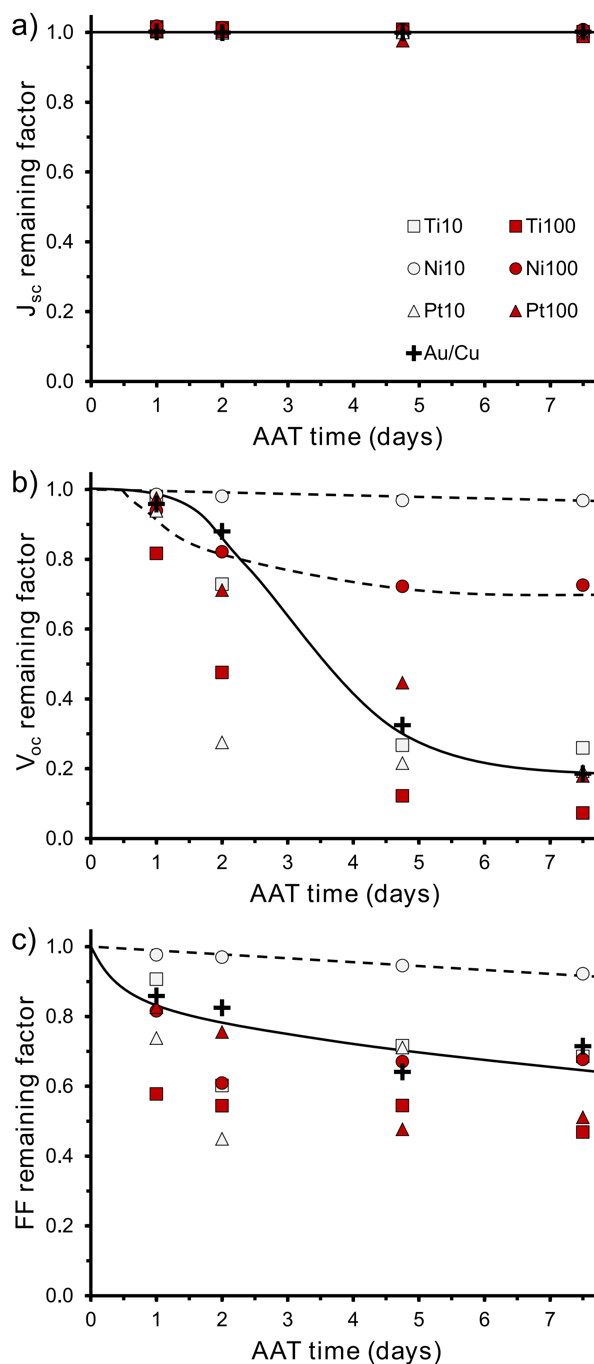

Fig. 3 Average a) J_{sc}, b) V_{oc} and c) FF remaining factors of cells with various front contact metallization schemes plotted versus AAT time at 250°C. The black lines indicate the general degradation trends of the Au/Cu cells and the dashed lines indicate the most notable deviations.

value of approximately 0.7. The Ti10, Ti100, Pt10 and Pt100 cells show degradation trends similar to or even (slightly) worse than the Au/Cu cells. This suggests that Ti and Pt are also unsuitable as barrier materials. The average results obtained (after 48 hours at 250°C) for the 100nm Ti barriers are significantly worse than obtained with the same metallization scheme in a previous study[42]. Closer analysis of the R-V_{oc} values of the individual Ti100 cells used in the current study shows that after 24 hours at 250°C two out of the four cells have an R-V_{oc} > 0.95, while the other two cells have an R-V_{oc} < 0.8. After 48 hours at 250°C these values have decreased to < 0.8 and < 0.3 respectively. This indicates that the moment that rapid degradation kicks in can differ significantly for the individual cells which hints that this degradation process had not yet started for the cells in the previous study. In this study Ni barriers show the largest potential as a Cu diffusion barrier for III-V solar cells. The most notable results are displayed

This journal is © The Royal Society of Chemistry [year]

by the Ni10 cells, which show virtually no decrease in J_{sc} and decreases of 3% and 8% in V_{oc} and FF respectively after 7.5 days at 250°C. Although the Ni100 cells show significantly more degradation than the Ni10 cells (R-V_{oc} values of 0.73 and 0.97 for the Ni100 and Ni10 cells respectively), the observed degradation is still far less severe than for Au/Cu cells (which show an average R-V_{oc} value of 0.19). The fact that the cells with thin Ni layers show less degradation than the cells with thick Ni layers indicates that these layers do not just act as a barrier that slows down the diffusion of Cu to the active cell structures but reduce the cell degradation via a different mechanism.

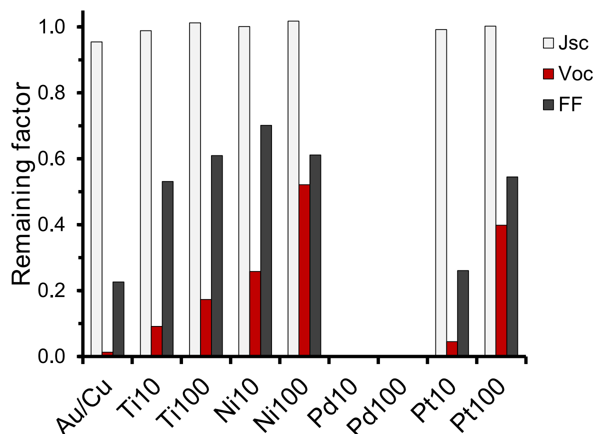

Fig. 4 Average J_{sc} (light grey bars), V_{oc} (red bars) and FF (dark grey bars) remaining factors for cells with various front contact metallization schemes after 5 hours AAT at 300°C.

In figure 4 the average J_{sc}, V_{oc} and FF remaining factors after 5 hours AAT at 300°C are plotted for cells with various front contact metallization schemes. Severe cell failure ($V_{oc} \approx 0$) was observed for cells with Pd barriers. Similar to the AAT results at 200 and 250°C the J_{sc} of the cells remains more or less constant. Large decreases in V_{oc} (R-V_{oc} < 0.55) and FF (R-FF < 0.70) are observed for all metallization schemes. All cells with barriers have (slightly) higher R-V_{oc} and R-FF values compared to cells without a diffusion barrier (Au/Cu) and cells with 100 nm thick barriers show (slightly) less degradation than cells with 10 nm thick barriers. This shows that at 300°C the barriers delay the degradation, but are unable to totally prevent severe device degradation.

3.2 Detailed assessment of Ni barriers

The results described in section 3.1 indicate that out of the investigated metals Ni offers the largest potential for application as a Cu diffusion barrier in III-V solar cells. In order to further study the barrier behaviour of 10 and 100 nm Ni barriers the J-V curves of Au/Cu, Ni10 and Ni100 metallization schemes were investigated in more detail. In figure 5 the J-V curves of Au/Cu, Ni10 and Ni100 cells are plotted after 37 days at 200°C (figure 5a), 7.5 days at 250°C (figure 5b) and 5 hours at 300°C (figure 5c), the curve of an as processed Au/Cu cell is plotted as a reference (the Ni10 and Ni100 cells initially had similar J-V characteristics). After AAT a reduction of V_{oc} results in the shift of the J-V curves towards the

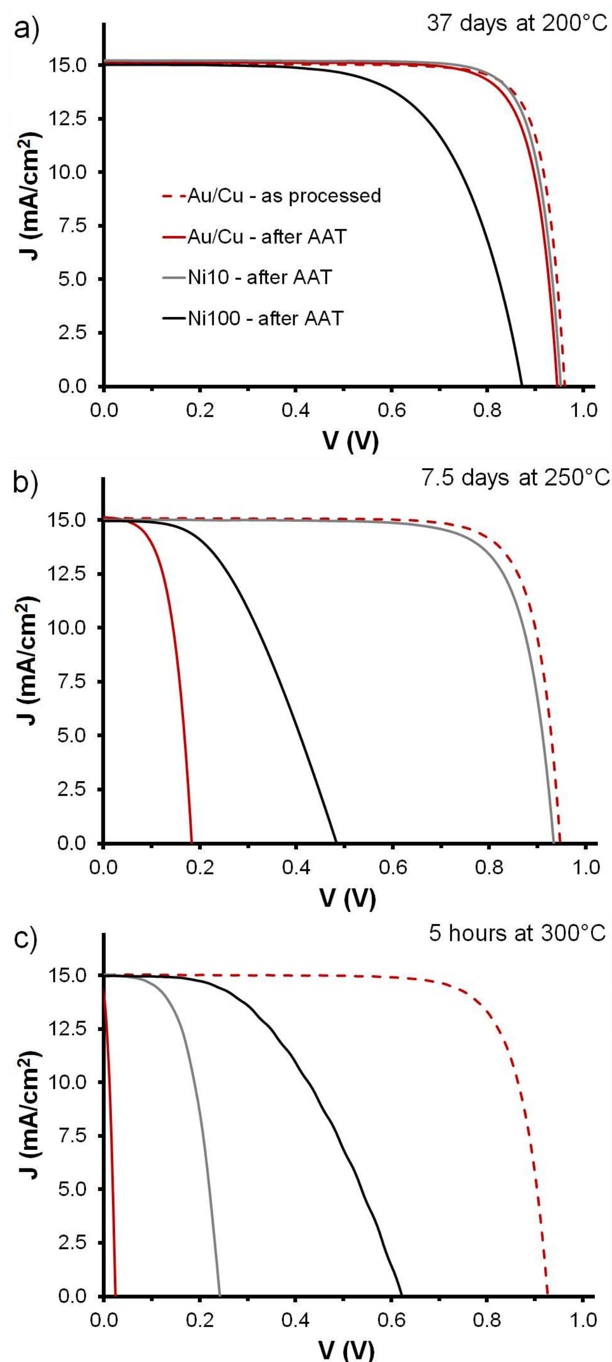

Fig. 5 J-V curves of Au/Cu, Ni10 and Ni100 cells (solid red, grey and black curves respectively) after a) 37 days at 200°C, b) 7.5 days at 250°C and c) 5 hours at 300°C. The curve of an as-processed Au/Cu cell is plotted as a reference (dashed red curve).

J axis. As V_{oc} can be approximated by[43]: $V_{oc} \approx \frac{kT}{q} \ln\left(\frac{J_{sc}}{J_0}\right)$ and J_{sc} changes very little, the decrease in V_{oc} must be caused by an increase in dark current density J_0. The most likely source of the increase in J_0 is increased (non-radiative) recombination via trap levels, which may be introduced by in diffusion of impurities such as Cu and Ni[16] or by introduction of other types of defects during AAT.

Additionally a clear increase in series resistance (R_S) is observed for the Ni100 cells (but not for the Ni10 cells) after AAT at all three temperatures. Series resistance effects are typically related to the contacts. Although Ni has a somewhat larger specific resistance than Au and Cu ($7.1*10^{-8}$, $2.3*10^{-8}$ and $1.7*10^{-8}$ Ω*m for Ni, Au and Cu respectively) the series resistance is not visible in the J-V curves of as-processed Ni100 cells, which indicates that it is not the presence of a thick (100 nm) Ni layer that causes the resistance effect. On the other hand alloys typically have higher resistances than the pure metals out of which they are formed, hence the increased R_S of Ni100 cells suggests that an interaction between the metals (and possibly the GaAs contact layer) takes place and that in this reaction an alloy, compound or structure is formed with a significantly higher specific resistance compared to the pure Ni layer. For cells with 10 nm Ni layers the thickness might be too small to form a coherent Ni alloyed layer or the effect on R_S is insufficient to be directly noticed in the J-V characteristics. As resistance effects typically result in decreases in FF, the increased series resistance of the Ni100 cells explains the drop in R-FF observed for these cells (see figures 2c, 3c and 4). Alternatively the decrease in FF may be caused by an increased contact resistance due to interaction between the GaAs contact layer and contact metals. This seems unlikely however, as the decrease in FF is already observed at 200°C and no interactions between the GaAs contact layer and the contact metals is expected at this temperature[20]. And secondly because such an interaction is also expected for the Au/Cu and Ni10 cells which do not show the increase in series resistance.

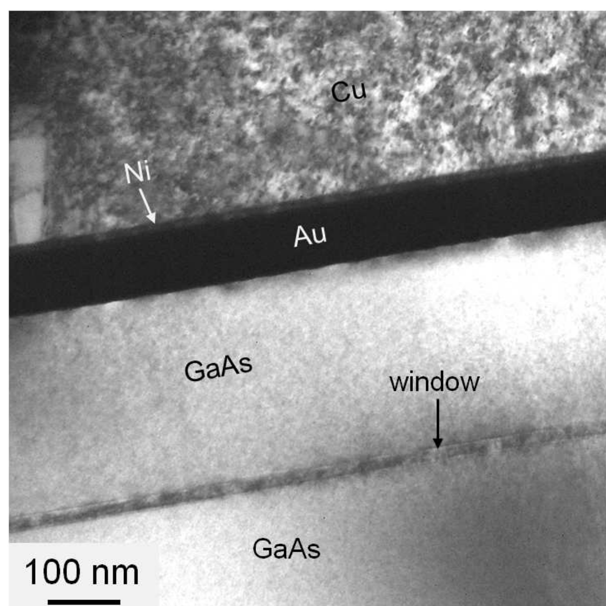

Fig. 6 TEM image of the front contact of an as processed cell with Ni10 metallization.

In order to further investigate the interactions taking place between the different layers of the front contact, cross-sectional TEM images of these contacts were prepared. In figure 6 a TEM image of the front contact of an as processed Ni10 cell is shown. This image clearly shows that before AAT the front contact consists of well defined layers of GaAs, Au, Ni and Cu with smooth interfaces in between, which is in agreement with the results previously obtained for cells with Au/Cu front contacts[20].

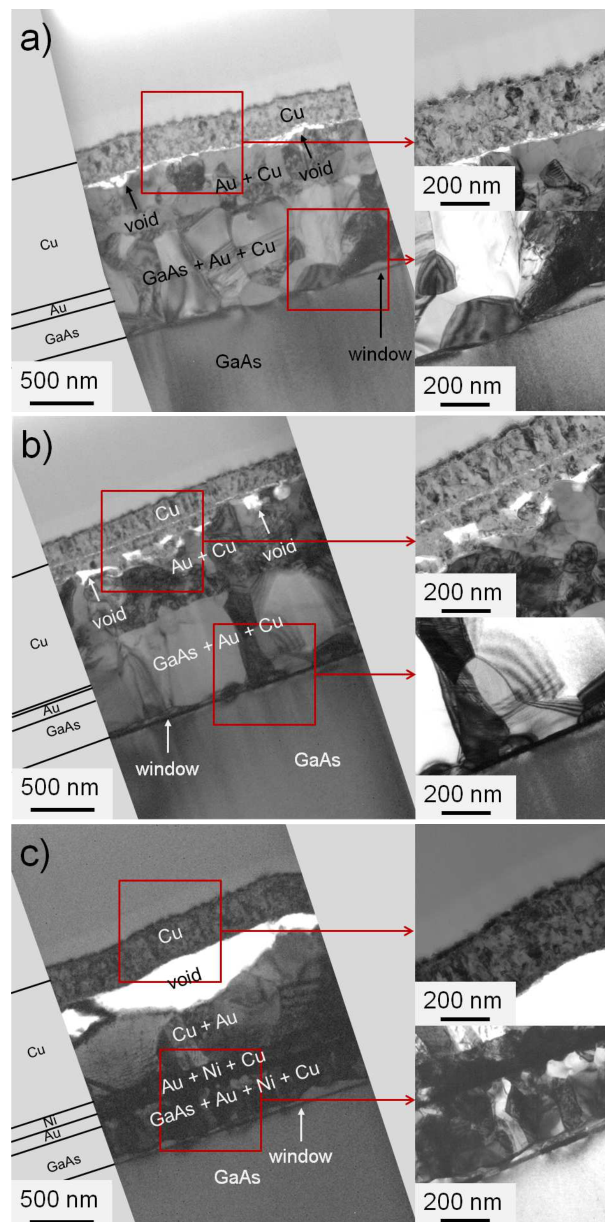

Fig. 7 TEM images of cells with a) Au/Cu b) Ni10 and c) Ni100 metallization after 7.5 days at 250°C. The black and grey text indicates the material composition as established by EDX, the solid black lines and text on the left hand side indicate the original layer structure of the as-processed cell. Images on the right hand side are enlargements of the top and bottom parts of the structures as indicated by the red squares.

As clear differences in degradation behaviour are observed at an AAT temperature of 250°C, cross-sectional TEM images of the front contacts of Au/Cu, Ni10 and Ni100 cells after 7.5 days of AAT at 250°C were prepared. These are shown in figure 7. The front contact of the Au/Cu cell (see figure 7a) shows a recrystal-

This journal is © The Royal Society of Chemistry [year]

lized GaAs/Au/Cu layer with an intermixed/recrystallized Au/Cu layer on top of it and a thin Cu layer at the front surface. The Cu and Au/Cu layers are separated by small voids. The formation of a recrystallized GaAs/Au/Cu layer and intermixed/recrystallized Au/Cu layer is in agreement with previously described mechanisms, as is the presence of a Cu layer at the surface [20]. However, the separation of the intermixed Au/Cu layer and Cu layer by voids was not observed in previous work in which the structures were only subjected to 4 hours of AAT compared to 7.5 days in the current study (compare figure 7a with figure 4c from [20]). This suggests that void formation starts later in the degradation process. The longer t_{acc} used in the current study also accounts for the progress in the recrystallization of the metals with the GaAs contact layer and hence the observed degradation in solar cell performance, as in diffusion of Cu via the grain boundaries in the recrystallized GaAs/Au/Cu layer is most likely responsible for the decrease in V_{oc} [20]. At some points the recrystallized GaAs/Au/Cu layer appears to have interacted with the window layer of the cell. If the window is actually penetrated this will increase the surface recombination velocity at the front side of the cell, yielding a reduced short circuit current density by a loss of blue response. The investigated cells, however, do not suffer from any loss in J_{sc} (see figure 3a) and their external quantum efficiencies before and after AAT are identical, indicating that the window is not penetrated and fully operational.

Surprisingly, at first glance the TEM images of the Ni10 cell (see figure 7b) appear to be remarkably similar to those of the cell without a barrier while their J-V characteristics (as shown in figure 5) are very different. Closer observation of the TEM images, however, reveals some small differences in the contact layer structure. Firstly, the grains in the recrystallized GaAs/Au/Cu layer appear to be somewhat larger in the lateral direction compared to the grains in the Au/Cu cell and secondly the intermixed Au/Cu layer appears to be more diffuse in the Ni10 cell. The larger (lateral) grain size may account for the relatively minor decrease in V_{oc} of Ni10 cells as larger grains imply that there are less grain boundaries via which Cu can diffuse into the cell. More likely, however, is that the 10 nm Ni acts as a so-called stuffed barrier [26]. In this mechanism the barrier atoms (in this case Ni) block the grain boundaries, thereby preventing diffusion. This diffusion of Ni into the grain boundaries complies well with the observation that the Ni10 cells do not show an increased R_S.

Compared to the cells without barrier and with 10 nm Ni barrier the cell with 100 nm Ni barrier shows a few remarkable differences. The voids between the intermixed Au/Cu layer and Cu layer are much larger and an additional Ni/Au/Cu layer is present between the recrystallized GaAs/Au/Cu layer and intermixed Au/Cu layer. The thickness and location of this additional layer suggest that the original 100 nm Ni (see left hand side of figure 7c) has formed a coherent Ni based alloyed layer, accounting for the increased R_S observed in these cells. This increase in R_S is not caused by the formation of large voids, since such void formation is also observed for Au/Cu and Ni10 cells after AAT at 300°C (see figure 8), which do not show a decrease in R_S. EDX analysis shows that Cu and Au are present at both sides of the Ni/Au/Cu layer which indicates that Ni does not act as a diffusion barrier in the sense that it prevents diffusion of Cu (and Au) across the barrier, but alters the degradation process in a different way.

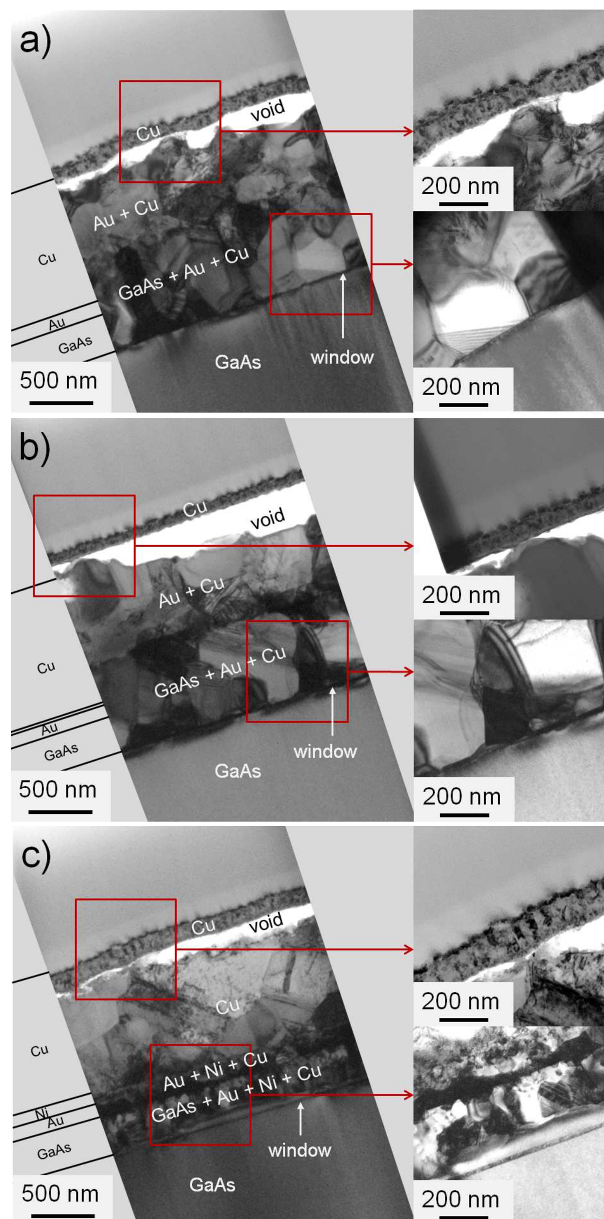

Fig. 8 TEM images of cells with a) Au/Cu b) Ni10 and c) Ni100 metallization after 5 hours at 300°C. The black and grey text indicates the material composition as established by EDX, the solid black lines and text on the left hand side indicate the original layer structure of the as-processed cell. Images on the right hand side are enlargements of the top and bottom parts of the structures as indicated by the red squares.

TEM images of the front contacts of Au/Cu, Ni10 and Ni100 cells after 5 hours of AAT at 300°C are shown in figure 8. The front contact of the Au/Cu cell shows a similar microstructure as after AAT at 250°C. The most notable differences are the thinner Cu layer and larger voids that have formed during AAT at 300°C. More significant differences in microstructure can be observed for

This journal is © The Royal Society of Chemistry [year]

the Ni10 cells. Similar to the Au/Cu cells a thinner Cu layer and larger voids have formed upon AAT at 300°C, but additionally the lateral grain size in the GaAs/Au/Cu layer is smaller after AAT at 300°C (compared to 250°C) and the intermixed Au/Cu layer has a grainy appearance which is quite different from the diffuse layer which has formed during AAT at 250°C. The front contact microstructure of the Ni100 cell after AAT at 300°C is similar to the Ni100 microstructure after AAT at 250°C. The most notable difference is the composition of the layer above the Ni/Au/Cu layer. EDX analysis shows that after 5 hours of AAT at 300°C this layer is composed solely out of Cu, whereas traces of Au are present after 7.5 days of AAT 250°C. This indicates that the presence of the Ni barrier significantly slows down the diffusion of Au into Cu, but not the diffusion of Cu into the Au (and GaAs) layer(s).

3.3 Barrier mechanism

The TEM images clearly show that the Ni layers do not act as a barrier in the classical sense (i.e. preventing diffusion of Cu and Au across the barrier), but that they reduce Cu related degradation by other mechanisms involving Ni diffusion and/or intermixing processes within the contact layer structure. Insight in these processes that ultimately reduce or prevent cell degradation in the AAT times relevant for the anticipated application can be obtained by combining the TEM analysis of the current and previous[20] study with information from (Cu, Ni, Au, Ga, As) phase diagrams reported in literature[44–50]. From these phase diagrams it can be concluded that (even at room temperature) Cu/Au, Cu/Ni, Ni/Au and Cu/GaAs interfaces are unstable, while Au/GaAs interfaces are stable. However, Kinsbron et al.[51] have found that at temperatures above ∼ 250°C Au/(Al)GaAs interfaces also become unstable.

In cells without a barrier two degradation mechanisms can be discerned[20]. At temperatures below ∼ 250°C the unstable Cu/Au interface results in gradual intermixing of the two materials. The Au/GaAs interface initially remains stable until the intermixed Cu/Au layer reaches the Au/GaAs interface. Then the presence of Cu destabilizes the interface and induces recrystallization of the GaAs contact layer with the metals. Once the recrystallized Cu/Au/GaAs layer approaches the window, Cu can diffuse rapidly into the active solar cell via the grain boundaries of the recrystallized layer. The fact that in a previous study[20] only mild undulation of the Au/GaAs interface was observed after 55 days at 200°C (equivalent to the extreme scenario of 15 years at 100°C at E_a = 0.70 eV) indicates that Cu diffusion via the grain boundaries is unlikely to occur within AAT times relevant for the anticipated application. The intermixing process also takes place at temperatures of 250°C and higher, but now at the same time the Au/GaAs interface becomes unstable as GaAs directly starts to decompose resulting in the out diffusion of As[51]. The Ga forms new phases with the Au, while the out diffusion of As potentially results in the formation of CuAs phases. This recrystallization process continues and Cu/Au/GaAs phases may be formed once the entire Au layer has either intermixed or recrystallized. Cu diffusion via the grain boundaries into the active solar can occur once the recrystallized GaAs/Au/Cu layer approaches the window layer.

In the presence of a Ni 'diffusion' barrier the unstable Au/Cu interface is replaced by two new interfaces: Au/Ni and Ni/Cu. Both these interfaces are unstable[48–50] thus intermixing is likely to occur. From the TEM images of the cells with 100 nm thick Ni barriers after AAT (figures 7c and 8c) it can be deduced that intermixing of Au and Ni dominates as the top and bottom edges of the intermixed Ni/Au/Cu layer appear to coincide with the original Au/GaAs and Ni/Cu interfaces. At temperatures below ∼ 250°C Au and Ni will gradually intermix to form an Au/Ni layer, while from the top small amounts of Cu diffuse into the layer as well. High Ni contents in this newly formed Ni/Au/Cu layer result in an increase in R_S, as can be observed in the J-V curves of the Ni100 cells (see figure 5). The Au/GaAs interface remains stable until Ni and/or Cu reach(es) the interface as a result of the intermixing of the metals. The metals can then recrystallize with the GaAs contact layer to form GaAs/Au/Ni/Cu phases. Once the recrystallized layer approaches the window rapid diffusion of Cu via the grain boundaries may occur, resulting in a decrease in V_{oc}. The fact that no significant drops in V_{oc} are observed after 37 days at 200°C (see figure 2b) indicates that recrystallization of the metals with the GaAs contact layer has not started yet or has not progressed sufficiently to facilitate Cu diffusion into the active layer of the cell. The fact that intermixing of Au, Ni and Cu still occurs indicates that Ni barriers are only suitable for application in substrate-based cells, as the intermixing process would diminish the mirror properties of the Au in thin-film cells[25].

At temperatures of ∼ 250°C and above additional diffusion/recrystallization/intermixing processes start to kick in, as the GaAs/Au interface becomes unstable, resulting in the decomposition of GaAs and recrystallization of GaAs with the contact metals. The TEM image of a Ni100 cell after 7.5 days at 250°C (see figure 7c) clearly shows that the GaAs contact layer has interacted with the metals. The relatively smooth interface between the recrystallized GaAs/metal layer and intermixed Ni/Au/Cu layer suggests that the presence of the intermixed metal layer to a certain extent confines the recrystallization process. The observed drop in V_{oc} (see figure 3b) indicates that Cu diffuses into the active solar cell region, but the fact that the decrease in V_{oc} is smaller than for a cell without barrier suggests that the presence of the intermixed Ni/Au/Cu layer slows down the diffusion process. The TEM image of the Ni10 cell (see figure 7b) shows that a 10 nm Ni barrier is not sufficient to confine the recrystallization of the GaAs layer. However, it appears that the presence of Ni allows for the formation of recrystallized grains with a relatively large lateral size, thereby reducing the number of grain boundaries and thus rapid Cu diffusion pathways. Possibly the Ni atoms also block the grain boundaries (acting as a stuffed barrier[26]). Increase of the AAT temperature to 300°C causes a more rapid proceeding of the different mechanisms, for the cells with 100 nm Ni barriers this does not affect the electrical performance and contact microstructure much, but the results for the cells with 10 nm Ni barriers are significantly different from the results at 250°C. Apparently the recrystallization process now proceeds fast enough to form a sufficient number of grain boundaries in the recrystallized layer. Thereby allowing Cu to diffuse to the window and into the active solar cell, where it induces a reduction in V_{oc}.

This journal is © The Royal Society of Chemistry [year]

4 Conclusions

In this study accelerated ageing testing (AAT), J-V characterization and TEM imaging in combination with phase diagram data from literature are used to assess the potential of Ti, Ni, Pd and Pt as diffusion barriers between the Au contact layer and Cu metallization of III-V solar cells. At all investigated temperatures (200-300°C) complete cell failure (V_{oc} virtually 0) was observed for the cells with Pd barriers, which indicates that Pd is totally unsuitable as a diffusion barrier. Cells with Ti and Pt barriers showed similar degradation behaviour as cells without a diffusion barrier and are therefore also expected to be unsuitable. On the other hand at an AAT temperature of 250°C cells with 10 and 100 nm thick Ni barriers show significantly better performance compared to Au/Cu cells. The Ni10 cells even show virtually no degradation after 7.5 days at 250°C (equivalent to 10 years at 100°C at an E_a of 0.70 eV). Detailed investigation shows that Ni does not act as a barrier in the classical sense, i.e. preventing diffusion of Cu and Au across the barrier. Instead Ni modifies or slows down the interactions taking place during device degradation and thus effectively acts as an 'interaction' barrier.

At relatively low temperatures (< 250°C) Ni, Au and Cu intermix. For low Ni fractions (originating from the thin Ni layers) this intermixing has no significant effect on the electrical performance of the cells, while at high Ni fractions (originating from the thick Ni layers) a significant increase in R_S is observed. Previous investigations in accordance to reported phase diagrams indicate that the GaAs contact layer of the cell will not start to recrystallize until the intermixing process has proceeded to such an extent that Cu reaches the GaAs interface to destabilize it.

The metal layer intermixing also occurs at higher temperatures (≥ 250°C), but at such temperatures decomposition of GaAs and out-diffusion of As immediately destabilizes the Au/GaAs interface , resulting in the direct initiation of the metal/GaAs recrystallization process. For a 100 nm thick Ni layer between Cu and Au the formation of a coherent Ni/Au/Cu layer upon AAT confines the recrystallization process of the GaAs contact layer and the metals. For thin (10 nm) Ni layers such confinement does not take place. TEM shows that the original Ni layer has totally disappeared while the average size of the crystals in the recrystallized layer appear to be larger. The highly reduced deterioration of cell with 10 nm Ni layers upon AAT can be explained by the lower density of grain boundaries in the recrystallized layers leading to a decrease in the Cu diffusion rate towards the active cell structure. In addition decoration of the grain boundaries with Ni resulting in a so-called stuffed barrier might further add to the observed increase of cell stability without suffering from an increase in R_S as obtained when thicker Ni layers are applied.

The results of this study indicate that 10-100 nm thick Ni intermediate layers in the Cu/Au based metallization of III-V solar cells may be beneficial to improve the device stability upon exposure to elevated temperatures. Further research is required to optimize the thickness of the Ni layers in relation to the actual temperature profile of the anticipated space applications.

Acknowledgements

The authors would like to thank Wil Corbeek for the technical support and Loes Scheers, Marlous Hofmans and Kiane de Kleijne for performing preparatory experiments with metal barriers. This project was financially supported by the Netherlands Space Office (NSO) under projectnumber PEP12010.

References

1 E. Yablonovitch, T. Gmitter, J. P. Harbison and R. Bnat, *Applied Physics Letters*, 1987, **51**, 2222–2224.

2 A. van Geelen, P. R. Hageman, G. J. Bauhuis, P. C. van Rijsingen, P. Schmidt and L. Giling, *Materials Science and Engineering*, 1997, **B45**, 162–171.

3 G. J. Bauhuis, J. J. Schermer, P. Mulder, M. M. A. J. Voncken and P. K. Larsen, *Solar Energy Materials & Solar Cells*, 2004, **83**, 81–90.

4 M. M. A. J. Voncken, J. J. Schermer, A. T. J. van Niftrik, G. J. Bauhuis, P. Mulder, P. K. Larsen, T. P. J. Peters, B. de Bruin, A. Klaassen and J. J. Kelly, *Journal of the Electrochemical Society*, 2004, **151**, G347.

5 M. M. A. J. Voncken, J. J. Schermer, G. J. Bauhuis, P. Mulder and P. K. Larsen, *Applied Physics A*, 2004, **79**, 1801–1807.

6 R. Tatavarti, G. Hillier, A. Dzankovic, G. Martin, F. Tuminiello, R. Navaratnajarah, G. Du, D. P. Vu and N. Pan, 33rd IEEE Photovoltaics Specialists Conference, 2008, pp. 1–4.

7 G. J. Bauhuis, P. Mulder, E. J. Haverkamp, J. C. C. M. Huijben and J. J. Schermer, *Solar Energy Materials & Solar Cells*, 2009, **93**, 1488–1491.

8 B. M. Kayes, H. Nie, R. Twist, S. G. Spruytte, F. Reinhardt, I. C. Kizilyalli and G. S. Higashi, Proceedings of the 37th IEEE Photovoltaics Specialists Conference, 2011.

9 S.-T. Hwang, S. Kim, H. Cheun, H. Lee, B. Lee, T. Hwang, S. Lee, W. Yoon, H.-M. Lee and B. Park, *Solar Energy Materials & Solar Cells*, 2016, **155**, 264–272.

10 J. J. Schermer, P. Mulder, G. J. Bauhuis, P. K. Larsen, G. Oomen and E. Bongers, *Progress in Photovoltaics: Research and Applications*, 2005, **13**, 587–596.

11 N. J. Smeenk, C. Mooney, J. Feenstra, P. Mulder, T. Rohr, C. O. A. Semprimoschnig, E. Vlieg and J. J. Schermer, *Polymer Degradation and Stability*, 2013, **98**, 2503–2511.

12 J. Feenstra, R. H. van Leest, N. J. Smeenk, P. Mulder, G. Oomen, E. Vlieg and J. J. Schermer, *Journal of Applied Polymer Science*, 2016, **133**, 43661.

13 E. Grossman and I. Gouzman, *Nuclear Instruments and Methods in Physics Research B*, 2003, **208**, 48–57.

14 C. S. Fuller and J. M. Whelan, *Journal of Physics and Chemistry of Solids*, 1958, **6**, 173–177.

15 R. N. Hall and J. H. Racette, *Journal of Applied Physics*, 1964, **35**, 379–397.

16 S. M. Sze and J. C. Irvin, *Solid-State Electronics*, 1968, **11**, 599–602.

17 N. Núñez, J. R. González, M. Vázquez, C. Algora and P. Espinet, *Progress in Photovoltaics: Research and Applications*, 2013, **21**, 1104–1113.

This journal is © The Royal Society of Chemistry [year]

18 N. Núñez, M. Vazquez, V. Orlando, P. Espinet-González and C. Algora, *Progress in Photovoltaics: Research and Applications*, 2015, **23**, 1857–1866.

19 ESA-ESTEC Requirements & Standards Division, *ECSS-E-ST-20-08C, Space Engineering: Photovoltaic assemblies and components*, 2012.

20 R. H. van Leest, K. de Kleijne, G. J. Bauhuis, P. Mulder, H. Cheun, H. Lee, W. Yoon, R. van der Heijden, E. Bongers, E. Vlieg and J. J. Schermer, *Physical Chemistry Chemical Physics*, 2016, **18**, 10232–10240.

21 R. H. van Leest, G. J. Bauhuis, P. Mulder, R. van der Heijden, E. Bongers, E. Vlieg and J. J. Schermer, *Solar Energy Materials & Solar Cells*, 2015, **140**, 45–53.

22 R. H. van Leest, K. de Kleijne, G. J. Bauhuis, P. Mulder, R. van der Heijden, E. Bongers, E. Vlieg and J. J. Schermer, Proceedings of the 31st European Photovoltaic Solar Energy Conference and Exhibition, 2015, pp. 1422–1425.

23 O. D. Miller, E. Yablonovitch and S. R. Kurtz, *IEEE Journal of Photovoltaics*, 2012, **2**, 303–311.

24 M. A. Steiner, J. F. Geisz, I. García, D. J. Friedman, A. Duda and S. R. Kurtz, *Journal of Applied Physics*, 2013, **113**, 123109.

25 R. H. van Leest, P. Mulder, N. Gruginskie, S. C. W. van Laar, G. J. Bauhuis, H. Cheun, H. Lee, W. Yoon, R. van der Heijden, E. Bongers, E. Vlieg and J. J. Schermer, *Accepted for publication: IEEE Journal of Photovoltaics*, –, **–**, –.

26 M.-A. Nicolet, *Thin Solid Films*, 1978, **52**, 415–443.

27 J. Kang, J. You, C. Kang, J. J. Pak and D. Kim, *Solar Energy Materials & Solar Cells*, 2002, **74**, 91–96.

28 J. You, J. Kang, D. Kim, J. J. Pak and C. S. Kang, *Solar Energy Materials & Solar Cells*, 2003, **79**, 339–345.

29 P. Vitanov, N. Tyutyundzhiev, P. Stefchev and B. Karamfilov, *Solar Energy Materials & Solar Cells*, 1996, **44**, 471–484.

30 E. J. Lee, D. Kim and S. H. Lee, *Solar Energy Materials & Solar Cells*, 2002, **74**, 65–70.

31 A. Mondon, M. N. Jawaid, J. Bartsch, M. Glatthaar and S. W. Glunz, *Solar Energy Materials & Solar Cells*, 2013, **117**, 209–213.

32 S. K. Min, D. H. Kim and S. H. Lee, *Electronic Materials Letters*, 2013, **9**, 433–435.

33 C. H. Lee, D. R. Kim and X. Zheng, *ACS Nano*, 2014, **8**, 8746–8756.

34 A. Kraft, C. Wolf, J. Bartsch, M. Glatthaar and S. Glunz, *Solar Energy Materials & Solar Cells*, 2015, **136**, 25–31.

35 M. C. Raval, A. P. Joshi, S. S. Saseendran, S. Suckow, S. Saravanan, C. S. Solanki and A. Kottantharayil, *IEEE Journal of Photovoltaics*, 2015, **5**, 1554–1562.

36 D. Tsunami, K. Nishizawa, T. Oka, T. Shiga, T. Oku and M. Takemi, *Palladium Diffusion Barrier Grown by Electroplating for backside Cu Metallization of GaAs devices*, http://www.csmantech.org/Digests/2013/papers/068.pdf, 2013, [Online; accessed 07 July 2014].

37 C.-H. Hsu, E. Y. Chang, H.-J. Chang, H. Yu, H. Q. Nguyen, J.-S. Maa and K. Pande, *IEEE Electron Device Letters*, 2014, **35**, 1275–1277.

38 C.-H. Hsu, E. Y. Chang, H.-J. Chang, J.-S. Maa and K. Pande, *Solid-State Electronics*, 2015, **114**, 174–177.

39 H. Ono, T. Nakano and T. Ohta, *Applied Physics Letters*, 1994, **64**, 1511–1513.

40 S.-Y. Jang, S.-M. Lee and H.-K. Baik, *Journal of Materials Science: Materials in Electronics*, 1996, **7**, 271–278.

41 C.-Y. Chen, L. Chang, E. Y. Chang, S.-H. Chen and D.-F. Chang, *Applied Physics Letters*, 2000, **77**, 3367–3369.

42 R. H. van Leest, G. J. Bauhuis, P. Mulder, K. de Kleijne, M. Hofmans, R. van der Heijden, E. Bongers, E. Vlieg and J. J. Schermer, Proceedings of the 43rd IEEE Photovoltaics Specialists Conference, 2016, pp. –.

43 M. A. Green, *Solar Cells*, Prentice-Hall, 1982.

44 H. Okamoto, D. J. Chakrabarti, D. E. Laughlin and T. B. Massalski, *Bulletin of Alloy Phase Diagrams*, 1987, **8**, 454–473.

45 P. P. Fedorov and S. N. Volkov, *Russian Journal of Inorganic Chemistry*, 2016, **61**, 772–775.

46 C. T. Tsai and R. S. Williams, *Journal of Materials Research*, 1986, **1**, 352–360.

47 R. Schmid-Fetzer, *Journal of Electronic Materials*, 1988, **17**, 193–200.

48 T. A. Hall and A. A. Johnson, *Journal of the Less-Common Metals*, 1988, **141**, L19–L22.

49 J. Mimkes and M. Wuttig, *Thermochimica Acta*, 1996, **282/283**, 165–173.

50 C. P. Wang, X. J. Liu, I. Ohnuma, R. Kainuma and K. Ishida, *Journal of Physics and Chemistry of Solids*, 2005, **66**, 256–260.

51 E. Kinsbron, P. Gallagher and A. T. English, *Solid-State Electronics*, 1979, **22**, 517–524.

This journal is © The Royal Society of Chemistry [year]